Hypervelocity impact induced deformation modes in α-alumina

Cheng Zhang, Rajiv K. Kalia, Aiichiro Nakano, and Priya Vashishta[a)]
Collaboratory for Advanced Computing and Simulations, Department of Chemical Engineering and Materials Science, Department of Physics and Astronomy, and Department of Computer Science, University of Southern California, Los Angeles, California 90089-0242

(Received 30 April 2007; accepted 5 June 2007; published online 13 August 2007)

Hypervelocity impact deformation mechanisms of α-alumina are studied using 540×10^6 atom molecular dynamics simulation on massively parallel computers. The projectile impact on the (0001) surface of α-alumina at 18 km/s exhibits a fundamentally different symmetry of the deformation patterns from those under lower strain rates. The simulation reveals a sequence of atomistic deformation mechanisms following localized melting and amorphization. These include pyramidal slips, basal slips and twins, rhombohedral twins, and twins along the $\{0\bar{1}11\}$. Some of these deformation patterns are not observed under lower impact velocities. © *2007 American Institute of Physics*. [DOI: 10.1063/1.2753092]

Ceramics have high melting/sublimation temperature and high values of hardness and compressive strength. They are widely used as protective shields against compressive loading. However, their ineffectiveness against hypervelocity impact, partly due to their low fracture toughness and low tensile strength, has been long studied to improve their performance in aircrafts and weapon systems. Recently, Subhash and Ravichandran have performed experiments to study the loading response of an AlN crystal under high strain rates.[1] Shih *et al.* have identified through experiments several deformation modes that lead to microcracks and eventual fracture in SiC.[2] Rosenberg *et al.*[3] and Mashimo *et al.*[4] have measured the dynamic compressive strength and elastoplastic properties of alumina; and Grady has measured its equation of state.[5] Karki *et al.* have investigated the compressive behavior of alumina as a constituent of earth mantle.[6] At the microscopic scale, research has been carried out to study deformation modes in ceramics, such as basal slip, pyramidal slip, prism plane slip, basal twin, and rhombohedral twin in alumina.[7–9] However, little is known about the atomistic deformation mechanisms at high strain rates. A powerful tool in identifying atomistic mechanisms of defects and fractures,[10,11] molecular dynamics (MD) simulation, has been employed to study material response under high strain rate loading.[12,13]

We report large-scale MD simulations focusing on nucleation, propagation, and interaction of deformations in α-alumina under hypervelocity impact. The simulation potential contains two-body and three-body terms[14] and has been validated against experimental values of mechanical quantities. The influence of deformation conditions, such as temperature and stress level, on deformation modes at the atomistic scale is investigated. Under such high strain rates, various deformation modes such as geometrically necessitated slip systems, which are inoperative under lower strain rate conditions, can be activated.

The simulated system is $200\times200\times130$ nm^3 in size containing 540×10^6 atoms, whose schematic is shown in Fig. 1. The substrate is impacted upon its top (0001) free surface by a projectile at impact velocity of 18 km/s. The impact surface is chosen to be along the crystalline plane of the highest symmetry. The projectile is a hexagonal cylinder of 20 nm wide and 40 nm long, whose interatomic potential is five times stiffer than normal alumina and atomic mass is fives times heavier. Absorbing boundary condition is applied on all sidewalls. The simulation lasts for approximately 30 ps until the substrate spalls on both top and bottom free surfaces. In order to study the effect of impact speed on deformation patterns, we have also performed simulation at 15 km/s.

Upon impact, large temperature and pressure gradients result in melting and amorphization of the substrate near the impact face. Temperature profile and diffusing behavior of the atoms directly in front of the impact face show that the substrate is melted in that region. To confirm the amorphized structure a little further away from the impact face, we have calculated the pair distribution and bond angle distribution

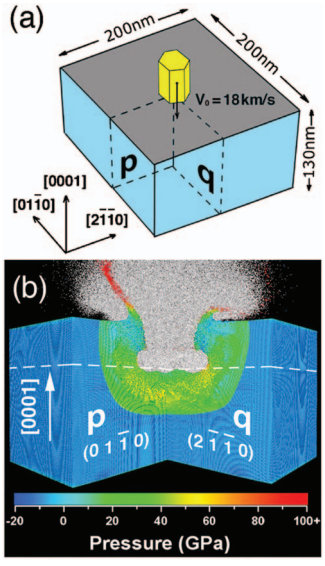

FIG. 1. (Color) (a) Schematic of the simulation setup. A rod impacts on the (0001) surface of α-alumina single crystal with a speed of 18 km/s. Deformations are visualized on the two major inner planes $\boldsymbol{p}$ $(01\bar{1}0)$ and $\boldsymbol{q}$ $(2\bar{1}\bar{1}0)$. (b) Pressure distribution at $t=5$ ps with inner surfaces $\boldsymbol{p}$ and $\boldsymbol{q}$ exposed. The dashed lines represent the basal plane at a depth of 40 nm, which is visualized in Fig. 2(a).

[a)]Electronic mail: priyav@usc.edu

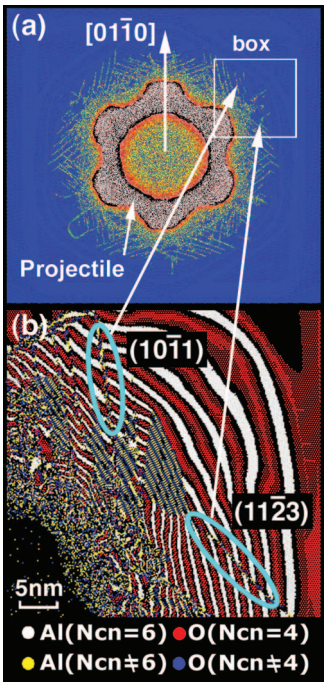

FIG. 2. (Color) (a) Snapshot of the substrate's cross section on the basal plane at a depth of 40 nm (the dashed line in Fig. 1(b)) and at 6 ps. Coordination numbers are used to color-code atoms. (b) A closeup of the boxed region color coded by atomic species, with two pyramidal slips circled out. Here N_{cn} is the coordination number of atoms.

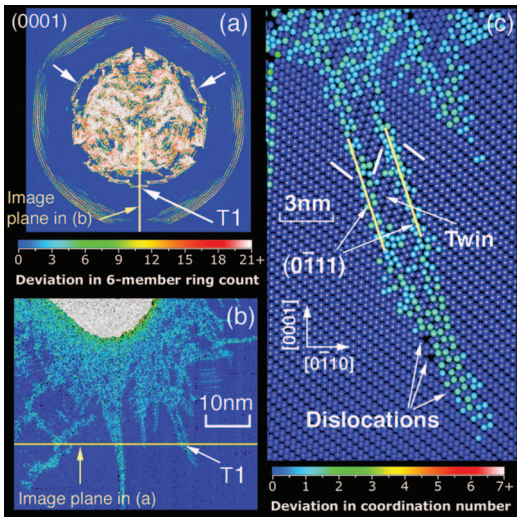

FIG. 3. (Color) (a) Ring analysis results in a basal slice of 40 nm in front of the projectile tip at 8 ps. T1, one of the twins (white arrows) along the $\{0\bar{1}11\}$, is on the boundary of a severely deformed region. It is also shown in (b), the center $(2\bar{1}\bar{1}0)$ plane (plane ***q*** defined in Fig. 1) view where atoms are color coded by their coordination numbers and the projectile atoms are colored in white. (c) A close-up image of (b) showing details of twin T1. The positions of the dislocations are determined by the misalignment of lattice planes.

functions locally and compare the data to those in bulk amorphous alumina that is prepared by a melt-quench method. The study shows that the amorphization is pressure driven, similar to the amorphization that Wentzcovitch *et al.*[15] have observed in silica. Outside the amorphized region, several modes of deformation mechanisms are observed in the substrate through coordination number and ring analysis.[16] An atom's coordination number refers to the number of nearest neighbors, while a ring refers to a shortest closed path through a neighbor atom triplet. These analyses are very effective in identifying deformation mechanisms.

At 3 ps, the amorphized region stops growing below the projectile and pyramidal slips nucleate at the amorphized region boundary. Figure 2(a) shows the 0001 cross section at a depth of 40 nm at 6 ps. The white-color region is the deformed projectile. The projectile penetrates the substrate deeper along the $\{2\bar{1}\bar{1}0\}$ since these are the weak planes under tensile loading.[17] From the impact fronts in the $\langle 01\bar{1}0\rangle$ directions, parallel streaks of pyramidal slips appear along four sets of orientations: $\{10\bar{1}1\}$, $\{\bar{1}012\}$, $\{2\bar{1}\bar{1}3\}$, and $\{4\bar{2}\bar{2}3\}$ [two of them are shown in the cyan ellipses in Fig. 2(b)]. Animation of the simulation shows that the slips initiate almost simultaneously and propagate with roughly constant speeds of up to 0.7 km/s. The higher shear stresses in the center cause inner dislocations to move faster and farther than outer ones. The slips eventually form concentric hexagrams in the basal plane before they stop each other at the intersections. All four slip planes ($\{10\bar{1}1\}$, $\{\bar{1}012\}$, $\{2\bar{1}\bar{1}3\}$, and $\{4\bar{2}\bar{2}3\}$) have been reported in previous experimental and theoretical studies,[18–20] which indicate that $\{10\bar{1}1\}$ and $\{2\bar{1}\bar{1}3\}$ pyramidal slips are energetically favorable than $\{\bar{1}012\}$ and $\{4\bar{2}\bar{2}3\}$. However, in our impact simulation, we observe equal amounts of pyramidal slips along all four planes. This is partly because each pyramidal slip family has only three possible orientations, while the shear stresses caused by projectile intrusion are more isotropic. Therefore, the energetically favorable slips alone cannot effectively relieve the shear stresses, which geometrically necessitates the presence of the other slips. Also the high temperature and high strain rate associated with hypervelocity impact provide sufficient energy to overcome the high activation barrier of the other slips. For impact simulation at 15 km/s, the pyramidal slips form similar six-fold pattern initially, which soon becomes three-fold as the slips along the $\{10\bar{1}1\}$ and $\{2\bar{1}\bar{1}3\}$ grow faster and farther than the other two slip systems.

By 6 ps, the projectile penetration has slowed down and amorphization has given way to deformations in the substrate. Figure 3 shows a basal plane snapshot in front of the projectile tip at 8 ps. A severely deformed region has formed in front of the projectile, which is roughly a cone with an opening angle of 40°. The deformed region is bounded by a series of twin deformations [arrows in Fig. 3(a)] propagating down from the projectile tip [a corner of the deformed projectile tip is shown in Fig. 3(b) as the white-colored region]. One of them, T1, is examined in Fig. 3(c) a close-up image of Fig. 3(b). It relieves the local shear stress from around 30 GPa on its left hand side to nearly 0 GPa on the right hand side, with a fixed width of ~1.5 nm. The twins advance at an approximately constant speed of 8 km/s all the way down to the bottom free surface with the maximum resolved shear stress of 17 GPa along the $\{0\bar{1}11\}$ around their tips.

A few picoseconds after the first series of twins form, more twins emerge outside the deformation cone surface near the three initial sites [arrows in Fig. 3(a)], along the $\{0\bar{1}12\}$ instead of the original $\{0\bar{1}11\}$ planes. When unloading wave[21] travels through, these twins cross slip to the $\{0\bar{1}11\}$ via basal planes and leave behind large amount of undercoordinated atoms and cavities. Such deformations are

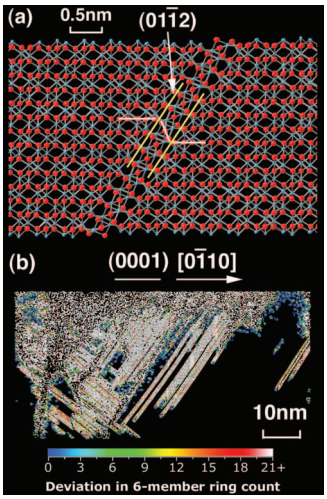

FIG. 4. (Color) (a) ($2\bar{1}\bar{1}0$) prism plane view of a rhombohedral twin. The red and blue spheres are oxygen and aluminum atoms, respectively. (b) The twinning region in a thin slice of prism plane (plane ***q*** defined in Fig. 1). The atoms are color coded if they have different numbers of six-member rings from perfect crystal. The streaks on the right are twins along the ($01\bar{1}2$), while the ones on the left running perpendicular are twins along the ($\bar{1}012$) and ($1\bar{1}02$).

not observed when the substrate is impacted at 15 km/s. In about 2 ps after the deformed region in Fig. 3(a) forms, a large number of rhombohedral twins emerge in the middle as the pressure is relieved. The atomic configuration around a twinning deformation in the simulation is shown in Fig. 4(a).

The atoms on the twin surfaces have normal coordination numbers (Al has 6 and O has 4). Viewed in the $[2\bar{1}\bar{1}0]$ direction, they appear as parallel long streaks along the $\{\bar{1}012\}$, as shown in Fig. 4(b). The width and spacing of the twins are multiples of 0.384 nm, which is equal to the $\{\bar{1}012\}$ interplanar spacing. As the $\{\bar{1}012\}$ has three possible orientations, twins of different orientations intersect to form a three-fold pattern. When they intersect, twins of different orientations stop each other and generate local disordered regions and cavities. Rhombohedral twins have been frequently observed in experiments.[22,23]

Most of the deformation modes are observed before 9 ps, when the shock wave reaches the bottom free surface. After 10 ps, unloading wave from the bottom free surface propagates through and causes large tension and shear in the substrate. Subsequently, large amount of basal deformations form on the boundary of the cone bounded by twins along the $\{0\bar{1}11\}$. The critical shear stress for the basal dislocation to advance is 15 GPa, whereas the theoretical value of Peierls stress is 17 GPa.[24] In contrast to the atomistically sharp slip surfaces of the twins, the basal slip surfaces are often more disordered. Both are among the most common deformation modes in α-alumina.[25,26] These are less frequently observed in the 15 km/s simulation.

In conclusion, our 540×10^6 atom MD simulation of hypervelocity impact on alumina shows that deformation modes are highly sensitive to the impact velocity and distinct from those under lower strain rates. The pyramidal slip systems along the $\{2\bar{1}\bar{1}3\}$, $\{10\bar{1}1\}$, $\{4\bar{2}\bar{2}3\}$, and $\{\bar{1}012\}$ have different activation energies but equal frequencies of occurrence in the simulation, which implies that their occurrences are geometrically necessitated by the six-fold stress distribution. Several twin systems emerge under different local conditions, such as rhombohedral twin, basal twin, and twin along the $\{0\bar{1}11\}$. The last one is unique and primarily responsible for the eventual failure of the substrate. The effect of substrate size on the deformation modes is negligible as the boundary reflection of loading wave trails those events.

This research was supported by NSF-ITR. (Grant Number DMR-0427188). Simulations were carried out at the University of Southern California HPCC facility and the 2048-processor Linux cluster at the Collaboratory for Advanced Computing and Simulations.

[1] G. Subhash and G. Ravichandran, J. Mater. Sci. **33**, 1933 (1998).
[2] C. J. Shih, M. A. Meyers, V. F. Nesterenko, and S. J. Chen, Acta Mater. **48**, 2399 (2000).
[3] Z. Rosenberg, D. Yaziv, Y. Yeshurun, and S. J. Bless, J. Appl. Phys. **62**, 1120 (1987).
[4] T. Mashimo, Y. Hanaoka, and K. Nagayama, J. Appl. Phys. **63**, 327 (1988).
[5] D. E. Grady, Mech. Mater. **29**, 181 (1998).
[6] B. B. Karki, L. Stixrude, and R. M. Wentzcovitch, Rev. Geophys. **39**, 507 (2001).
[7] A. H. Heuer, K. P. D. Lagerlöf, and J. Castaing, Philos. Mag. A **78**, 747 (1998).
[8] J. Castaing, A. He, K. P. D. Lagerlöf, and A. H. Heuer, Philos. Mag. **84**, 1113 (2004).
[9] S. J. Chen and D. G. Howitt, Philos. Mag. A **78**, 765 (1998).
[10] J. Li, K. J. Van Vliet, T. Zhu, S. Yip, and S. Suresh, Nature (London) **418**, 307 (2002).
[11] F. F. Abraham, J. Q. Broughton, N. Bernstein, and E. Kaxiras, Europhys. Lett. **44**, 783 (1998).
[12] B. L. Holian, Shock Waves **5**, 149 (1995).
[13] K. Kadau, T. C. Germann, P. S. Lomdahl, and B. L. Holian, Science **296**, 1681 (2002).
[14] P. Vashishta, R. K. Kalia, A. Nakano, and J. P. Rino, J. Appl. Phys. **101**, 103515 (2007).
[15] R. M. Wentzcovitch, C. da Silva, J. R. Chelikowsky, and N. Binggeli, Phys. Rev. Lett. **80**, 2149 (1998).
[16] C. Zhang, B. Bansal, P. S. Branicio, R. K. Kalia, A. Nakano, A. Sharma, and P. Vashishta, Comput. Phys. Commun. **175**, 339 (2006).
[17] The six-fold symmetry formed by the weak planes is not a direct consequence of the projectile's geometry because it initially has six corners aligned along the $\langle 2\bar{1}\bar{1}0\rangle$.
[18] R. E. Tressler and D. J. Barber, J. Am. Ceram. Soc. **57**, 13 (1974).
[19] J. Cadoz and B. Pellissier, Scr. Metall. **10**, 597 (1976).
[20] D. M. Kotchick, B. J. Busovne, R. E. Tressler, and D. J. Barber, J. Mater. Sci. **17**, 1977 (1982).
[21] After the shock wave emanating from the impact point reaches the back free surface of the target, it is reflected back as a tensile unloading wave.
[22] T. Geipel, K. P. D. Lagerlöf, P. Pirouz, and A. H. Heuer, Acta Metall. Mater. **42**, 1367 (1994).
[23] B. J. Inkson, Acta Mater. **48**, 1883 (2000).
[24] K. P. D. Lagerlöf, A. H. Heuer, J. Castaing, J. P. Riviere, and T. E. Mitchell, J. Am. Ceram. Soc. **77**, 385 (1994).
[25] J. Castaing, A. Munoz, D. G. Garcia, and A. D. Rodriguez, Mater. Sci. Eng., A **233**, 121 (1997).
[26] H. M. Chan and B. R. Lawn, J. Am. Ceram. Soc. **71**, 29 (1988).